ACS SENSORS

pubs.acs.org/acssensors Article

Colorimetric Detection of SARS-CoV-2 and Drug-Resistant pH1N1 Using CRISPR/dCas9

Jeong Moon, Hyung-Jun Kwon, Dongeun Yong, In-Chul Lee, Hongki Kim, Hyunju Kang, Eun-Kyung Lim, Kyu-Sun Lee, Juyeon Jung,* Hyun Gyu Park,* and Taejoon Kang*

Cite This: https://dx.doi.org/10.1021/acssensors.0c01929 Read Online

ACCESS | Metrics & More | Article Recommendations | Supporting Information

ABSTRACT: Viruses have been a continuous threat to human beings. The coronavirus disease 2019 (COVID-19), caused by severe acute respiratory syndrome coronavirus 2 (SARS-CoV-2), has led to a pandemic that is still ongoing worldwide. Previous pandemic influenza A virus (pH1N1) might be re-emerging through a drug-resistant mutation. We report a colorimetric viral detection method based on the clustered regularly interspaced short palindromic repeats (CRISPR)/Cas9 endonuclease dead (dCas9) system. In this method, RNA in the viral lysate was directly recognized by the CRISPR/dCas9 system with biotin-protospacer adjacent motif (PAM)-presenting oligonucleotide (PAMmer). Streptavidin-horseradish peroxidase then bound to biotin-PAMmer, inducing a color change through the oxidation of 3,3′,5,5′-tetramethylbenzidine. Using the developed method, we successfully identified SARS-CoV-2, pH1N1, and pH1N1/H275Y viruses by the naked eye. Moreover, the detection of viruses in human nasopharyngeal aspirates and sputum was demonstrated. Finally, clinical samples from COVID-19 patients led to a successful diagnosis. We anticipate that the current method can be employed for simple and accurate diagnosis of viruses.

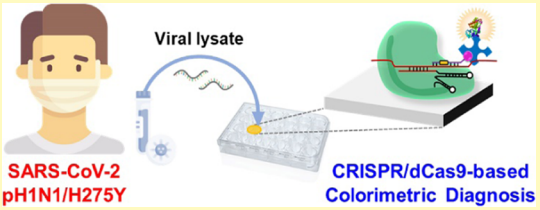

KEYWORDS: *SARS-CoV-2, COVID-19, drug-resistance, influenza virus, CRISPR/dCas9, colorimetry*

Infectious diseases have been a great threat to human beings over the past several decades.[1,2] They are spreading globally faster and appear to be emerging quicker than at any other time in history.[1,2] Particularly, viruses such as pandemic influenza A virus (pH1N1), severe acute respiratory syndrome coronavirus (SARS-CoV), Middle East respiratory syndrome coronavirus, Ebola virus, and Zika virus have caused severe infectious diseases in the 21st century.[1,2] Now, coronavirus disease 2019 (COVID-19) caused by SARS-CoV-2 infection has become an unprecedented threat to global health.[1,2] Currently, over fifty-three million cases of SARS-CoV-2 have been identified, and more than a million deaths from COVID-19 have been reported around the world.[3] Although several drug and vaccine candidates are being developed, and no clear strategy has yet been reported as a treatment for COVID-19 patients.[4] Moreover, while the SARS-CoV-2 pandemic is still ongoing, concerns are emerging simultaneously over the seasonal influenza virus (IFV) epidemic. Therefore, it is recommended that viruses are quickly and accurately diagnosed for the proper treatment as well as prevention of the spread of SARS-CoV-2.[5,6]

After the emergence, spread, and even declaration of the end of a viral infection, the potential threat remains for the re-emergence of mutant viruses. In 2009, an outbreak of pH1N1 infection occurred in the United States and approximately 60.8 million cases, 274 304 hospitalizations, and 12 468 deaths were reported from April 12, 2009, to April 10, 2010.[7] Following the outbreak of pH1N1, oseltamivir has been the most widely used treatment for patients infected with the influenza virus (IFV).[8−10] However, new drug-resistant mutant viruses have emerged due to the abuse of oseltamivir, and these mutant viruses have become a potential threat to public health.[8−10] Considering that oseltamivir is the most frequently used drug for the treatment of patients with IFV infection, the diagnosis of oseltamivir-resistant viruses is of great importance in the treatment of IFV-infected patients.[8−10]

SARS-CoV-2 has been predominantly diagnosed by quantitative reverse transcription-polymerase chain reaction (qRT-PCR) approaches.[11] These methods take at least 4−6 h and require a complicated viral RNA extraction step that can affect diagnostic accuracy.[12] Serological tests can be used for the diagnosis of SARS-CoV-2 infected patients; however, the tests are limited to the late diagnosis of COVID-19 patients because it takes several days for the patient to develop a detectable amount of antibodies after the onset of symptoms.[13−15] Meanwhile, drug-resistant viruses have mainly been detected by nucleotide sequencing after PCR, and

Received: September 15, 2020
Accepted: November 19, 2020

https://dx.doi.org/10.1021/acssensors.0c01929
ACS Sens. XXXX, XXX, XXX−XXX

recently advanced sensing techniques have been developed by employing novel chemical and biological receptors.[8−10] Consequently, a rapid, simple, and accurate molecular diagnostic method in response to new and re-emerging viral threats is urgently required.

The clustered regularly interspaced short palindromic repeats (CRISPR) associated nuclease (Cas) (CRISPR/Cas) system is an ancient bacterial immune system against foreign genetic material.[16] The system harbors a programmable protein that can cut DNA or RNA, enabling bacteria to become resistant to foreign genes.[16] These days, the CRISPR/Cas system has been advanced into a sophisticated gene-editing technique.[17] Since the report that the CRISPR/Cas system can be used for the detection of nucleic acids, several fascinating disease diagnostic methods have been developed such as CRISPR-based diagnostic SHERLOCK and DETECTR, CRISPR-mediated DNA FISH, CRISPR-dCas9-immobilized on a graphene field-effect transistor, CRISPR-Cas9-triggered strand displacement amplification method, functional RNA regulated CRISPR-Cas12a sensor, and CRISPR/Cas13a-powered electrochemical sensor.[12,18−25] Compared to conventional PCR-based methods, CRISPR-based diagnostic approaches have several advantages including high specificity due to enzymatic recognition of the target nucleic acid, fast turnaround time, convenient isothermal reaction, and wide applicability due to the simple programmable system.[26] Simultaneously, colorimetric biosensing techniques detecting target molecules by naked eyes or simple portable optical detectors have attracted attention because of their simplicity, practicality, and cost-effectiveness.[27,28] These advantages allowed us to develop a simple colorimetric virus detection method using the CRISPR/Cas system and apply this method for the diagnosis of SARS-CoV-2 and oseltamivir-resistant pH1N1.

Herein, we report a CRISPR/dCas9 system-based viral diagnostic method and successful detection of SARS-CoV-2, pH1N1, and pH1N1/H275Y mutant viruses. Guide RNAs (gRNAs) were designed to recognize each virus, and dCas9/gRNA complexes were immobilized on a well microplate. For the colorimetric detection of SARS-CoV-2, pH1N1, and pH1N1/H275Y, viral lysates and biotin-protospacer adjacent motif (PAM)-presenting oligonucleotide (PAMmer) were added to dCas9/gRNA-attached well plates, followed by the horseradish peroxidase (HRP)/3,3′,5,5′-tetramethylbenzidine (TMB) reaction. Using this method, SARS-CoV-2, pH1N1, and pH1N1/H275Y viruses were successfully detected with the naked eye. In addition, viruses in human nasopharyngeal aspirates and sputum were identified. Finally, clinical samples from five COVID-19 patients were accurately diagnosed as positive. The developed method enabled us to detect infectious viruses simply and precisely because it has the advantages of viral lysate detection, naked-eye perception, isothermal reaction, and single nucleotide polymorphism (SNP) selectivity. We anticipate that the current method can be useful for the accurate diagnosis of viruses, preventing the spread of infectious diseases.

EXPERIMENTAL SECTION

Materials and Reagents. RNA oligonucleotides purified by RNase-free high-performance liquid chromatography, gRNA, and recombinant *Streptococcus pyogenes* dCas9 protein (1081067) were purchased from Integrated DNA Technologies, Inc. (Coralville, IA). The 10× FastDigest buffer, Dulbecco's modified Eagle' medium (DMEM), and antibiotic-antimycotic were purchased from Thermo Fisher Scientific (Waltham, MA). GelRed nucleic acid stain (41003) was purchased from Biotium (Hayward, CA). Phosphate-buffered saline (PBS), Tween 20, bovine serum albumin (BSA), streptavidin-HRP (18−152), diethyl pyrocarbonate-water, and tosyl phenylalanyl chloromethyl ketone (TPCK) trypsin were purchased from Sigma-Aldrich (St. Louis, MO). Tris(2-carboxyethyl)phosphine (TCEP) was purchased from LPS Solution (Daejeon, Korea). Ethylenediaminetetraacetic acid (EDTA) solution was purchased from Dynebio (Seongnam-si, Gyeonggi-do, Korea). The TMB substrate reagent set (555214) was purchased from BD Biosciences (San Jose, CA). SARS-CoV-2 (BetaCoV/Korea/KCDC03/2020) and pH1N1/H275Y mutant virus (H275Y mutation; A/Korea2785/2009 pdm: NCCP 42017) were provided by the National Culture Collection for Pathogens (NCCP), which is operated by the Korea National Institute of Health. pH1N1 virus (A/California/07/2009) was obtained from the BioNano Health Guard Research Center (H-GUARD) of Korea.

Binding Test of RNA and Biotin-PAMmer with the dCas9/gRNA Complex. The dCas9/gRNA ribonucleoprotein (RNP) complex was prepared by incubating 100 nM gRNA and 1 μM dCas9 in 100 μL of PBS for 10 min at 25 °C. The prepared RNP complexes (10, 50, 100, and 250 nM) and target RNA (1 μM) were mixed with biotin-PAMmer (1 μM) and then incubated in 20 μL of 1× FastDigest buffer for 1 h at 37 °C. After the addition of 6× DNA loading buffer, 20 μL of each reaction product was loaded onto 8% native polyacrylamide gel for electrophoresis. Finally, the gel was stained with GelRed and visualized using a Gel Doc XR+ Gel System (Bio-Rad Laboratories, Hercules, CA).

dCas9/gRNA RNP Complex Immobilization Test Using ELISA. The dCas9/gRNA RNP complex was constructed by incubating 600 nM gRNA and 1 μM dCas9 in 100 μL of PBS for 10 min at 25 °C. After 10 times dilution of the RNP complex, 100 μL of diluted RNP complex solution was incubated in a 96-well microplate for 2 h at 25 °C. Afterward, the well surfaces were washed with washing buffer (1× PBS containing 0.05% Tween 20) three times. To prevent nonspecific binding, 0.1 mg/mL BSA was added to the well surfaces and incubated for 40 min at 25 °C. After washing the surfaces with washing buffer, anti-Cas9 monoclonal antibody (Guide-it Cas9 Monoclonal Antibody #632628, Takara Bio USA, Inc., Mountain View, CA) and secondary antibody conjugated with HRP (Goat Anti-Mouse IgG (H+L)-HRP Conjugate #1706516, Bio-Rad Laboratories, Inc.) were sequentially added. Lastly, TMB substrate reagents and 2.5 M sulfuric acid were added to the surfaces.

Colorimetric RNA Detection Using CRISPR/dCas9. The dCas9/gRNA RNP complex was constructed by incubating 600 nM gRNA and 1 μM dCas9 in 100 μL of PBS for 10 min at 25 °C. After 10 times dilution of the RNP complex, 100 μL of diluted RNP complex solution was incubated in a 96-well microplate for 2 h at 25 °C. Afterward, the well surfaces were washed with washing buffer (1× PBS containing 0.05% Tween 20) three times. To prevent nonspecific binding, 0.1 mg/mL BSA was added to the well surfaces and incubated for 40 min at 25 °C. After washing the surfaces with the washing buffer, 10 μL of target RNA was incubated for 60 min at 37 °C in a final 100 μL of 1× FastDigest buffer containing 1 μM biotin-PAMmer. Next, the well surfaces were washed with washing buffer, and 1 μg/mL of streptavidin-HRP was added for 30 min at 25 °C. Finally, TMB substrate reagents and 2.5 M sulfuric acid were sequentially added onto the surfaces. Optical density (OD) was measured using Cytation 5 Multi-Mode Reader (BioTek, Winooski, VT).

Colorimetric Virus Detection Using CRISPR/dCas9. SARS-CoV-2 was propagated in Vero cells (ATCC No. CCL-81) in DMEM without fetal bovine serum with 1% antibiotic-antimycotic and TPCK trypsin (final concentrations of 0.5 μg/mL) at 37 °C and 5% CO_2 for 72 h. The propagated viruses were stored at −80 °C for future use. Infectious virus titers were determined by 50% tissue culture infective dose ($TCID_{50}$) in confluent cells in 96-well microplates. All experiments using SARS-CoV-2 were performed at the Korea Centers for Disease Control and Prevention (KCDC)-approved Biosafety

https://dx.doi.org/10.1021/acssensors.0c01929
ACS Sens. XXXX, XXX, XXX−XXX

Level 3 (BL-3) facility of Korea Research Institute of Bioscience and Biotechnology (KRIBB) in accordance with institutional biosafety requirements. pH1N1 and pH1N1/H275Y virus titers were determined using a one-step real-time PCR kit (Promega, Madison, WI) in accordance with the manufacturer's instructions. For the preparation of viral lysates, 90 μL of virus samples were treated with 10 μL of TCEP/EDTA (final concentrations of 100 and 1 mM, respectively) and heated at 50 °C for 5 min and 64 °C for 5 min. The dCas9/gRNA-coated microplates were prepared as described above. A total of 60 μL of viral lysate was added to the dCas9/gRNA-coated surfaces and incubated for 60 min at 37 °C in a final 100 μL of 1× FastDigest buffer containing 1 μM biotin-PAMmer. Next, the well surfaces were washed with the washing buffer, and 1 μg/mL of streptavidin-HRP was added for 30 min at 25 °C. Lastly, TMB substrate reagents and 2.5 M sulfuric acid were sequentially added onto the surfaces. The OD was measured as described above.

Nasopharyngeal aspirates and sputum samples from patients were collected with flocked nasopharyngeal swabs and placed into the virus transport media (UTM, Copan Diagnostics Inc., Murrieta, CA). All samples were stored at −70 °C until use. The protocol for this retrospective study was reviewed and approved by the Institutional Review Board of Yonsei University Health Service Center, Severance Hospital, Seoul, Korea (IRB approval number: 4-2020-0465). To detect the virus in human nasopharyngeal aspirates and sputum, 10 μL of the virus was spiked into 90 μL of the human nasal fluid sample. The virus concentration was 10^2 PFU/mL. The virus in human fluid (90 μL) was then treated with 10 μL of TCEP/EDTA (final concentrations of 100 and 1 mM, respectively) and heated at 50 °C for 5 min and 64 °C for 5 min. The next detection procedures were the same as above.

Diagnosis of COVID-19 Patients Using CRISPR/dCas9. Nasopharyngeal aspirates and sputum samples from COVID-19 patients were collected and stored as described above. For the detection of SARS-CoV-2 in nasopharyngeal aspirates and sputum of patients, 90 μL of the clinical sample was treated with 10 μL of TCEP/EDTA (final concentrations of 100 and 1 mM, respectively) and heated at 50 °C for 5 min and 64 °C for 5 min. The next detection procedures were the same as above.

RESULTS AND DISCUSSION

Colorimetric RNA Detection Using CRISPR/dCas9. Figure 1 shows a schematic illustration of virus detection based on the CRISPR/dCas9 system. The dCas9 protein forms a RNP complex with gRNA.[29] The gRNA, which contains a complementary sequence to the target sequence, confers specificity to the CRISPR/dCas9 system.[29] Prepared dCas9/gRNA RNP complexes are attached to a microplate.

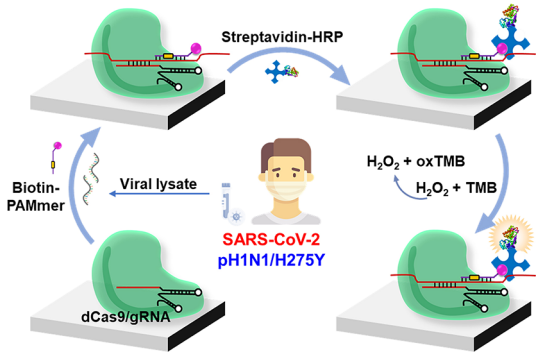

Figure 1. Schematic illustration of virus detection based on CRISPR/dCas9. Viral lysate and biotin-PAMmer are added into a dCas9/gRNA complex-immobilized microplate. Next, streptavidin-HPR and TMB substrate solutions are added to the microplate. Finally, yellow color is observed in the presence of the virus.

Next, the viral lysate and biotin-PAMmer were added to the RNP-attached microplate. After incubation and washing, streptavidin-HRP and TMB reagents were added to the plate and washed. As a result, yellow color was observed in the presence of the viral RNA corresponding to gRNA. The total assay can be conducted within 90 min. This method adopted a dCas9/gRNA complex for the recognition of target RNA and the HRP/TMB reaction for colorimetric detection. Previous studies have revealed that the dCas9/gRNA complex can bind to RNA in a programmed manner with a PAMmer.[30] PAM is a DNA sequence immediately following the DNA sequence targeted by the Cas9 nuclease.[30] The presence of PAMmer is important for the exclusive recognition of the target RNA using the CRISPR/dCas9 system because the Cas9 target search mechanism relies on the PAM sequence.[30] We designed PAMmer sequences that can hybridize to the target RNAs of SARS-CoV-2, pH1N1, and pH1N1/H275Y viruses (Table S1). Moreover, biotin was added to the 3′-termini of the PAMmer sequence, allowing the binding of streptavidin-HRP. Since the HRP/TMB reaction has been extensively used in biochemical applications,[31] it is feasible to identify the presence of the virus with the naked eye or by simple measurement of OD. Compared to microchips or microarrays that have to be analyzed indirectly by cDNA amplification and need sophisticated hybridization conditions between the capture probe and target molecule,[32] the proposed dCas9/gRNA-based RNA detection method can directly and easily detect target RNAs without cDNA amplification.

Before the detection of target RNA using the CRISPR/dCas9 system, we initially examined the binding ability of the dCas9/gRNA complex to the RNA with biotin-PAMmer using a gel mobility shift assay. The sequences of gRNA, target RNA, and biotin-PAMmer are displayed in Figure S1a. Figure S1b shows the electrophoretic mobility shift in the presence of the target RNA/biotin-PAMmer hybrid with the dCas9/gRNA complex (0, 10, 50, 100, and 250 nM). As the concentration of dCas9/gRNA increased, a large number of target RNA and biotin-PAMmer hybrids were combined with the dCas9/gRNA complex. From this result, it was demonstrated that dCas9/gRNA RNP could recognize target RNA and biotin-PAMmer. The surface immobilization of dCas9/gRNA was also confirmed using enzyme-linked immunosorbent assay (ELISA). As shown in Figure S2, it was identified that the dCas9/gRNA RNP could be successfully attached to the surfaces of the well plate. In addition, the optimal concentrations of RNP, biotin-PAMmer, and HRP-streptavidin were established as 0.1, 1 μM, and 1 μg/mL, respectively, by comparing the OD values under various conditions (Figure S3).

For the detection of SARS-CoV-2 using the CRISPR/dCas9 system, gRNA and biotin-PAMmer sequences were designed according to the SARS-CoV-2 N1, N2, and N3 genes (Figures S4a and S5a,c). The gRNA and PAMmer regions were selected based on primer sequences provided by the Centers for Disease Control and Prevention (CDC).[11] Each gRNA was designed to target 20 nucleotides within the sequence of the SARS-CoV-2 N1, N2, and N3 genes, and each PAMmer was composed of a 5′-extension and a mismatched PAM. In addition, eight nucleotides were extended in the 5′ direction from the PAM site to improve the specificity of PAMmer.[33] Figure 2a shows the plot of the $OD_{450\ nm}$ value as a function of SARS-CoV-2 N1 RNA concentration. As the concentration of RNA increased from 0.1 to 100 nM, the $OD_{450\ nm}$ value also

https://dx.doi.org/10.1021/acssensors.0c01929
ACS Sens. XXXX, XXX, XXX−XXX

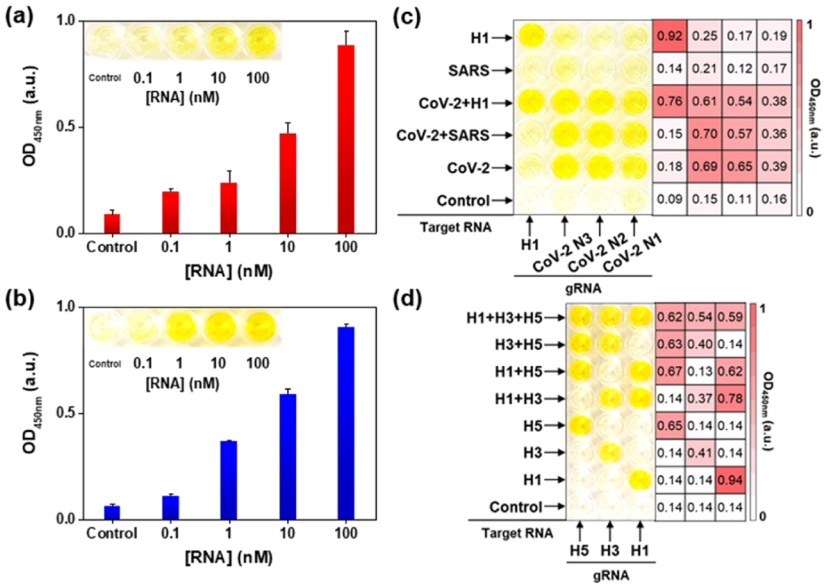

Figure 2. (a) Plot of $OD_{450\ nm}$ versus the concentration of SARS-CoV-2 N1 RNA (0, 0.1, 1, 10, and 100 nM). Inset is a photograph of the microplate after the detection of SARS-CoV-2 N1 RNA using CRISPR/dCas9. (b) Plot of $OD_{450\ nm}$ versus the concentration of pH1N1 H1 RNA (0, 0.1, 1, 10, and 100 nM). Inset is a photograph of the microplate after the detection of pH1N1 H1 RNA using CRISPR/dCas9. (c, d) Photographs of microplates and corresponding heat maps after the detection of various RNAs using CRISPR/dCas9. gRNA and target RNA are written at the bottom and left side of the microplates, respectively. CoV-2 is a mixture of SARS-CoV-2 N1, N2, and N3 target RNAs. SARS is SARS-CoV target RNA. H1, H3, and H5 are pH1N1 H1, influenza A H3, and influenza A H5 target RNAs, respectively. Only in the presence of the target RNA corresponding to gRNA, the color of dCas9/gRNA-immobilized wells turns yellow. The concentrations of the target RNA used for (c) and (d) are 10 and 100 nM, respectively.

increased. The linearly fitted line equation was $y = 0.145x + 0.354$, where y is the $OD_{450\ nm}$ value and x is the RNA concentration (Figure S4b). The limit of detection (LOD) was estimated to be 140 pM, following the equation $LOD = 3s_b/m$, where s_b is the standard deviation of the response of the control and m is the slope of the calibration curve. The inset is a photograph of a microplate after the detection of SARS-CoV-2 N1 RNA using the CRISPR/dCas9 system. The higher the concentration of RNA, the more distinct the yellow color was observed. We also tried to detect SARS-CoV-2 N2 and N3 RNAs using a microplate attached to dCas9/gRNA and successfully observed color changes in the presence of target RNAs (Figure S5b,d). Figure S4c shows the sequences of gRNA, pH1N1 H1, and biotin-PAMmer for the detection of pH1N1. The sequences were designed based on the primer information publicly provided by the World Health Organization (WHO).[34] The pH1N1 H1 RNA was detectable using the CRISPR/dCas9 system, as shown in Figure 2b. The color of the well surfaces turned yellow in the presence of the target RNA, and the corresponding $OD_{450\ nm}$ value increased as the concentration of pH1N1 H1 RNA increased. The linearly fitted line equation was $y = 0.171x + 0.368$, where y is the $OD_{450\ nm}$ value and x is the RNA concentration (Figure S4d). The LOD was estimated to be 30 pM. This suggested that RNAs of SARS-CoV-2 and pH1N1 can be recognized using the CRISPR/dCas9-based detection method.

The use of well microplates is beneficial for the simultaneous detection of several target molecules.[35] We prepared well surfaces attached with four kinds of dCas9/gRNA (CoV-2 N1, N2, N3, and H1) complexes and investigated the selective detection of several target RNAs. Figure 2c shows a photograph of the microplate and the corresponding heat maps after the detection of various target RNA mixtures (10 nM) using the CRISPR/dCas9 RNP system. The control sample showed no signal from any of the dCas9/gRNA-attached wells. When the target RNA mixture of SARS-CoV-2 N1, N2, and N3 (CoV-2) was tested, the surface of the three wells on the right turned yellow. When the mixture of SARS-CoV and CoV-2 RNAs was added into a dCas9/gRNA-attached well plate, the same right three well surfaces were yellow because the gRNA for the SARS-CoV sequence was absent on the microplate. These results suggest that the simultaneous and accurate detection of SARS-CoV-2 N1, N2, and N3 genes is feasible, allowing precise diagnosis of SARS-CoV-2. All four wells exhibited a distinct yellow color in the presence of CoV-2 and H1 RNAs. Conversely, no signals were observed from SARS-CoV RNA, and the left single well only exhibited a yellow color from the H1 RNA. This proved that accurate RNA recognition was possible using the developed approach. The heat map of the $OD_{450\ nm}$ value further confirmed that the current method can specifically detect the target RNA in the mixture. Figure 2d shows a photograph of the microplate and the corresponding heat map after identifying the IFV subtype using the CRISPR/dCas9 system. IFV subtyping has been considered a critical tool in the diagnosis and treatment of influenza because antiviral resistance is associated with the type of viral strain.[36] As shown in Figure 2d, three types of dCas9/gRNA (H1, H3, and H5) complex-immobilized well surfaces were prepared, and combinational mixtures of target RNAs (100 nM) were tested. In the presence of a single kind of target RNA, each matched well surface exhibited a yellow color. When two types of target RNA were examined, the corresponding two well surfaces indicated distinct color perceptions. From the mixture of H1, H3, and H5 RNAs, all three well surfaces were yellow in color. The control sample showed no color change. The heat map of the $OD_{450\ nm}$ value also supported the accurate subtyping of IFV RNAs. Based on these results, we concluded that the

https://dx.doi.org/10.1021/acssensors.0c01929
ACS Sens. XXXX, XXX, XXX−XXX

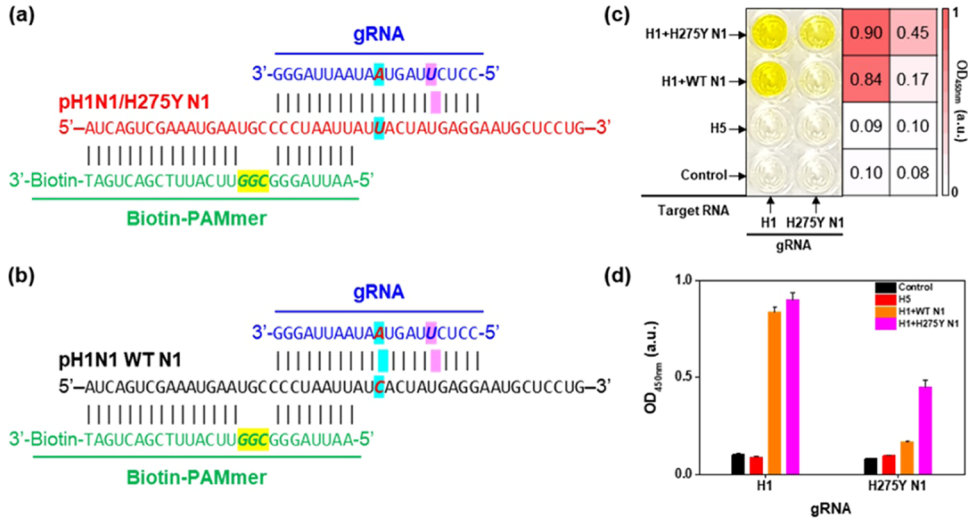

Figure 3. (a, b) Sequence of gRNA, pH1N1/H275Y N1, pH1N1 WT N1, and biotin-PAMmer. (c) Photograph of microplate and corresponding heat map after detection of various RNAs using CRISPR/dCas9. gRNA and target RNA are written at the bottom and left side of the microplate, respectively. Only in the presence of pH1N1 H1 and pH1N1/H275Y N1 RNAs, the color of both wells turns yellow. (d) Plot of $OD_{450\ nm}$ versus gRNA after the detection of various RNAs using CRISPR/dCas9. The concentrations of target RNAs are 100 nM.

CRISPR/dCas9-based method enabled us to specifically detect the target RNA. CRISPR/dCas9 can easily be reprogrammed by simply changing the sequence of gRNA; however, the on-target activity and off-target effects can vary widely depending on the individual gRNA.[37] Therefore, the target specificity of the CRISPR/dCas9 system can be improved when combined with an appropriate gRNA optimization process.[37]

The H275Y amino acid substitution of neuraminidase (NA) is the most common mutation in the N1 subtype of IFV, conferring oseltamivir resistance.[8−10] Since the first emergence of the pH1N1/H275Y mutant virus, the occurrence of mutant viruses has sharply increased, posing a threat to global public health.[8−10] Nevertheless, it has been difficult to identify the mutant virus routinely because the NA H275Y mutation of IFV is caused by a SNP.[38] For the detection of the pH1N1/H275Y mutant virus, we designed gRNA, as shown in Figure 3a. The gRNA sequence was matched to the pH1N1/H275Y N1 gene, including the SNP (italic and sky-blue background in Figure 3a) but mismatched those of pH1N1 wild-type (WT) N1 gene (italic and sky-blue background in Figure 3b). Moreover, we intentionally spiked an additional mismatched gRNA sequence against both WT and H275Y N1 RNAs (italic and magenta background in Figure 3a,b). This mismatched sequence is five bases away from the H275Y SNP and plays an important role in the precise recognition of the H275Y SNP. Without the spiked mismatched gRNA sequence, the gRNA perfectly matched the pH1N1/H275Y RNA and single mismatched to pH1N1 WT RNA (Figure S6a). In this case, H275Y N1 RNA was clearly detected with the naked eye, and WT N1 RNA was also recognizable (Figure S6b). By adding a mismatched gRNA sequence, the H275Y SNP could be distinguished using the CRISPR/dCas9 system. Similar strategies for SNP identification have been employed in previous studies.[23] Figure 3c is a photograph and the corresponding heat map after the detection of H275Y N1 RNA. The dCas9/gRNA (H1)- and dCas9/gRNA (H275Y N1)-attached well microplates were prepared, and several target RNAs (100 nM) were investigated. The control and H5 samples showed no color on both well surfaces. When the mixture of H1 and WT N1 target RNAs was added to the wells, only the dCas9/gRNA (H1)-attached surface showed a distinct yellow color. When testing the mixture of H1 and H275Y N1 RNAs, both well surfaces exhibited a yellow color, implying the successful identification of the H275Y SNP. Figure 3d shows a plot of the $OD_{450\ nm}$ value versus the type of gRNA, further confirming the identification of the pH1N1/H275Y mutation. The well-designed gRNA enabled us to distinguish the pH1N1/H275Y SNP.

Colorimetric Virus Detection Using CRISPR/dCas9. After the evaluation of the CRISPR/dCas9-based RNA detection method, we tried to detect SARS-CoV-2 and pH1N1 using the CRISPR/dCas9 system. SARS-CoV-2 was provided by the Korea National Institute of Health and was cultured in a BL-3 laboratory of the KRIBB. For the detection of SARS-CoV-2 and pH1N1, viral samples were treated with a lysis buffer and heated. Next, viral lysates were added to the dCas9/gRNA-coated well surfaces in the presence of biotin-PAMmer. After incubation, washing, and immersion of streptavidin-HRP and TMB reagents, the color and $OD_{450\ nm}$ value of the microplate were observed. Figure S7 shows the detection results of SARS-CoV-2 and pH1N1 using dCas9/gRNA-immobilized microplates, indicating that 10 PFU/mL of viruses could be distinguished from the control sample. More importantly, we demonstrated the simultaneous detection of SARS-CoV-2 and pH1N1 on a CRISPR/dCas9-immobilized plate (Figure 4a). As shown in Figure 4b, four types of dCas9/gRNA-attached well surfaces were prepared. The left column of the microplate was modified with dCas9/gRNA (H1) for pH1N1, and the three right columns were modified with dCas9/gRNA (CoV-2 N1, N2, and N3) for SARS-CoV-2. When the control sample was tested, no signal was observed from the surface of the four wells. When the viral lysate of SARS-CoV-2 was immersed, the surfaces of the three wells on the right exhibited a yellow color. On all four types of well surfaces the color signals were turned on after the detection of the SARS-CoV-2 and pH1N1 mixtures. Finally, the left single well surface showed the color change only in the presence of pH1N1. Although a slight cross-reaction was observed between pH1N1 and SARS-CoV-2 due to the internal off-target activity of the CRISPR/Cas9 system,[39] the heat map

https://dx.doi.org/10.1021/acssensors.0c01929
ACS Sens. XXXX, XXX, XXX−XXX

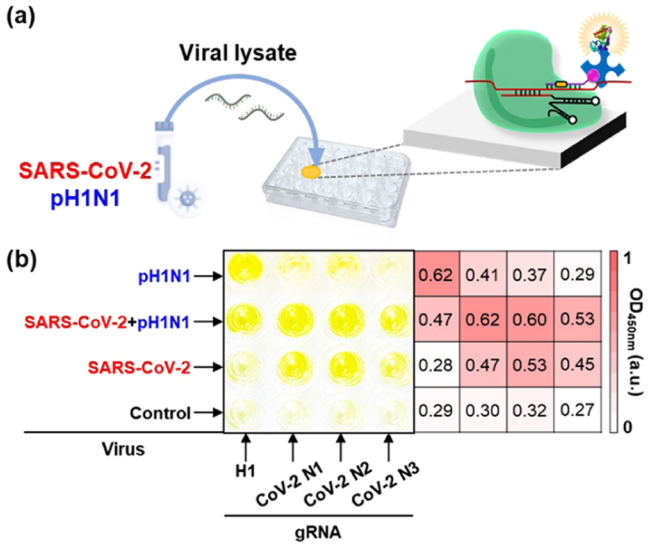

Figure 4. (a) Schematic illustration of SARS-CoV-2 and pH1N1 detection based on CRISPR/dCas9. (b) Photograph of microplate and corresponding heat map after the detection of viruses using CRISPR/dCas9. gRNA and the target virus are written on the bottom and left side of the microplate, respectively. Only in the presence of the virus corresponding to gRNA, the color of dCas9/gRNA-immobilized wells turns yellow. The virus concentrations are 10^3 PFU/mL.

results showed that the multiplex detection of virus mixture was feasible using this CRISPR/dCas9-based system. Recently, it was reported that the CRISPR-based nucleic acid method is suitable for massively multiplexed detection.[40] Moreover, it is noteworthy that SARS-CoV-2 and pH1N1 were detectable using viral lysates without RNA extraction and amplification processes, which can affect the accuracy of viral diagnosis. This advantage can be attributed to the accurate sequence recognition properties of the CRISPR/dCas9 system.

Viruses, including SARS-CoV-2 and pH1N1, have been mainly collected from patients using nasopharyngeal and oropharyngeal swabs. Therefore, we tried to detect viruses in human nasopharyngeal aspirates and sputum samples (Figure 5a). The human fluid samples were provided by Yonsei University Health Service Center, Severance Hospital of Korea, after the approval of the institutional review board (IRB). To detect SARS-CoV-2 in human fluid samples, SARS-CoV-2 was spiked in human nasopharyngeal aspirates and sputum samples. The SARS-CoV-2 in human fluid samples was then lysed by the addition of the lysis buffer and heating. Next, the human nasopharyngeal aspirates and sputum samples containing lysed viruses were directly applied to the CRISPR/dCas9 system. The virus concentration was 10^2 PFU/mL. Figure 5b shows a photograph and corresponding heat map after the detection of SARS-CoV-2-spiked human nasopharyngeal aspirates and sputum samples. The yellow color was observed from all well surfaces regardless of the type of gRNA (CoV-2 N1, N2, and N3), indicating the successful detection of SARS-CoV-2 in human fluids. Conversely, weak signals were obtained from control nasopharyngeal aspirates and sputum samples (Figure 5c). Based on this result, it is anticipated that an on-site diagnosis of SARS-CoV-2 would be feasible using the developed approach. We further investigated the identification of pH1N1 and pH1N1/H275Y mutant viruses in human nasopharyngeal aspirates and sputum samples. As shown in Figure 5d, upper well surfaces were coated with dCas9/gRNA (H1) and lower with dCas9/gRNA (H275Y N1). When testing the control human fluid samples, the color of the well plate was preserved, and the corresponding heat map also indicated sparse color (left panel in Figure 5d). The middle panel in Figure 5d shows a photograph and heat map after the detection of pH1N1-spiked human fluid samples, providing a distinct yellow color only from the dCas9/gRNA (H1)-immobilized well surfaces. When the pH1N1/H275Y virus-spiked human nasopharyngeal aspirates and sputum samples were examined, the color signals turned on at both the dCas9/gRNA (H1)- and dCas9/gRNA (H275Y N1)-attached well surfaces. The results show that the H275Y mutation in IFV can be identified using the developed CRISPR/dCas9 system. We expect that the CRISPR/dCas9-based method can be used for antiviral drug-resistant influenza virus diagnostic tests as well as COVID-19 patient diagnostic tests.

Diagnosis of COVID-19 Patients Using CRISPR/dCas9.

Finally, we tested nasopharyngeal aspirates and sputum samples collected from five COVID-19 patients using the developed CRISPR/dCas9 system. The samples were acquired from Yonsei University Health Service Center, Severance Hospital of Korea from March 6 to April 3, 2020, and diagnosed positive for COVID-19 using qRT-PCR (Table S2). Similar to the SARS-CoV-2 spike test above, the lysed virus samples were added to the dCas9/gRNA (CoV-2 N1, N2, and N3)-immobilized microplates and the detection procedure was performed. Figure 6 shows the photograph and corresponding heat map after the detection of SARS-CoV-2 in nasopharyngeal aspirates (Nos. 1, 2, and 5) and sputum (Nos. 3 and 4) samples collected from COVID-19 patients. All five clinical samples exhibited a yellow color on the dCas9/gRNA-attached well surfaces. The control nasopharyngeal aspirate samples (Nos. 6–8) showed sparse color. This result suggested that the CRISPR/dCas9 system can be used for the diagnosis of COVID-19 patients.

Currently, the emergence of COVID-19 patients is mainly driven by local community transmission.[41] South Korea was the host to the first large outbreak of COVID-19 outside of China.[42] However, cases of COVID-19 in South Korea dropped sharply, and no new domestic infection cases were reported on April 30.[42] This was the result of massive COVID-19 testing and strict self-discipline. Unfortunately, local infections in South Korea were newly reported on May 7, and cases of COVID-19 infections are increasing again.[42] This situation clearly underscores the importance of simple diagnostic tests for SARS-CoV-2. The developed approach is advantageous for the simple detection of SARS-CoV-2 because of the use of viral lysate without RNA extraction, pre-amplification, on-site colorimetric detection without huge equipment, isothermal reaction, and SNP specificity (Table S3). Despite its advantages, the multistep approach, sensitivity, and quantification of this method are limited compared to the PCR-based method. However, we suppose that there is an urgent need for simple SARS-CoV-2 detection, such as the current method. Furthermore, the color perception of this method is identical to that of the well-known ELISA method. Since we are developing a novel antibody against SARS-CoV-2, and soon, it will be possible to develop a simultaneous molecular and immunological diagnostic method for SARS-CoV-2 by combining the current approach with a new antibody.

https://dx.doi.org/10.1021/acssensors.0c01929
ACS Sens. XXXX, XXX, XXX−XXX

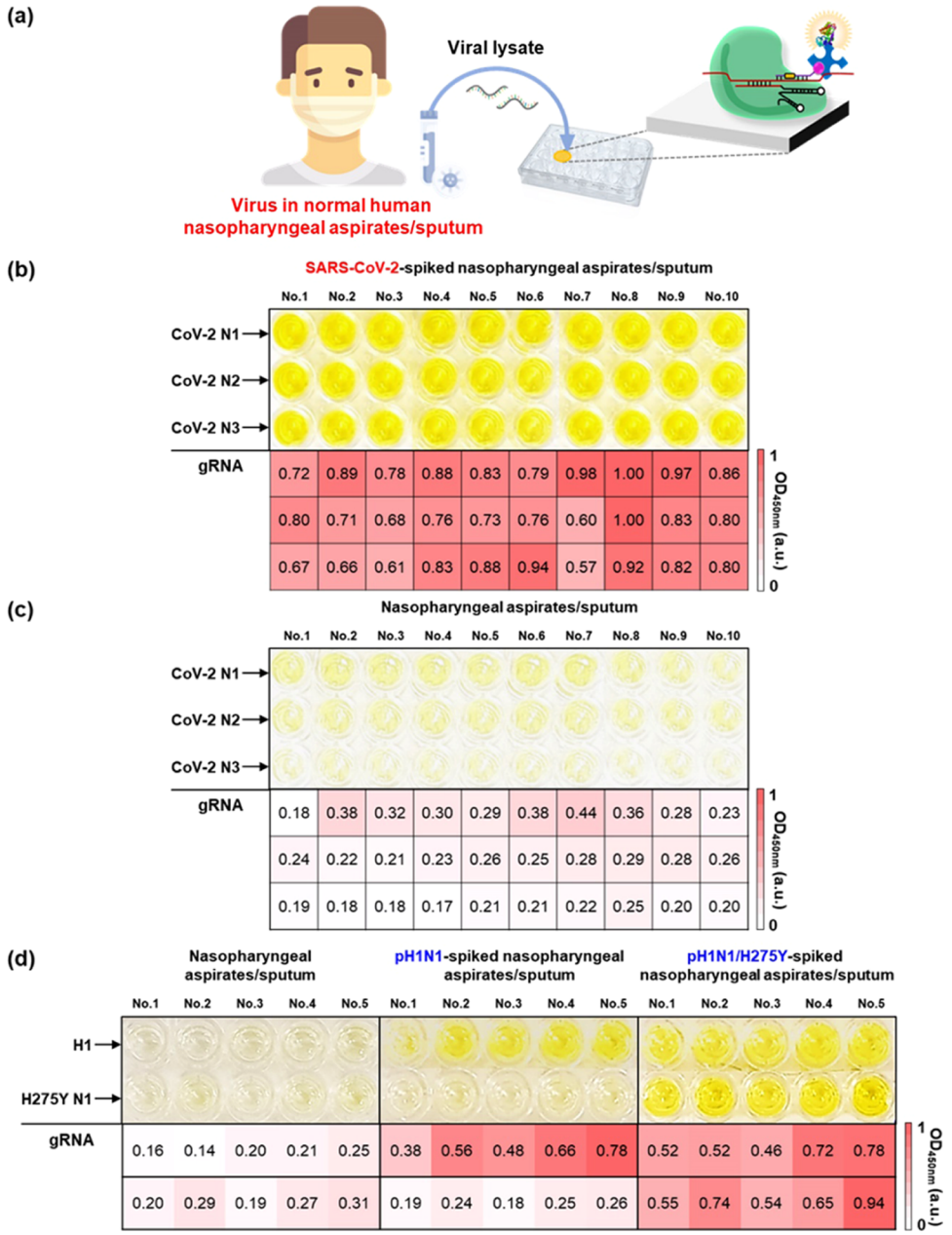

Figure 5. (a) Schematic illustration of virus detection in human nasopharyngeal aspirates and sputum samples based on CRISPR/dCas9. (b, c) Photographs of microplates and corresponding heat maps after the detection of SARS-CoV-2-spiked and control human fluid samples using CRISPR/dCas9. gRNA is written on the left side of the microplates. Only in the presence of SARS-CoV-2, the color of dCas9/gRNA-attached wells turns yellow. (d) Photograph of the microplate and corresponding heat map after the detection of pH1N1-spiked, pH1N1/H275Y-spiked, and control human fluid samples using CRISPR/dCas9. gRNA is written on the left side of the microplate. In the presence of pH1N1, the color of dCas9/gRNA (H1)-attached wells turns yellow. In the presence of pH1N1/H275Y, the color of all dCas9/gRNA (H1 and H275Y N1)-attached wells turns yellow.

CONCLUSIONS

In summary, a colorimetric viral detection method was developed using the CRISPR/dCas9 system. RNA in the viral lysate was recognized by the dCas9/gRNA RNP complex with biotin-PAMmer, and then the streptavidin-HRP/TMB reaction enabled the colorimetric detection of the virus. We evaluated the method using RNAs of SARS-CoV-2 N1, N2, and N3, pH1N1 H1, and pH1N1/H275Y N1 genes. In addition, viruses including SARS-CoV-2, pH1N1, and oseltamivir-resistant pH1N1/H275Y were successfully detected in dCas9/gRNA-immobilized well microplates. For the use of this method for clinical samples, virus-spiked human nasopharyngeal aspirates and sputum samples were tested, and distinct color changes were observed in the presence of SARS-CoV-2, pH1N1, and pH1N1/H275Y mutant viruses. Furthermore, attempts were made to diagnose clinical samples collected from the COVID-19 patients, and the identification of SARS-CoV-2 with the naked eye was successful. It is anticipated that a simple CRISPR/dCas9-based virus detection method can be useful for the diagnosis of current COVID-19 patients as well as re-emerging drug-resistant viruses in the future.

https://dx.doi.org/10.1021/acssensors.0c01929
ACS Sens. XXXX, XXX, XXX−XXX

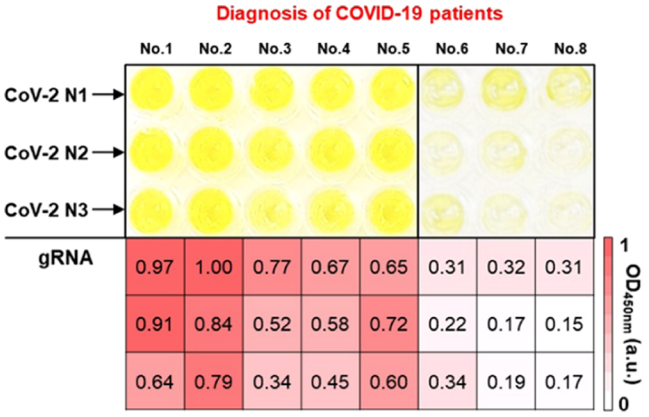

Figure 6. Photograph of microplate and the corresponding heat map after the detection of SARS-CoV-2 in clinical samples using CRISPR/dCas9. Left five samples were collected from positively diagnosed COVID-19 patients and right three samples were from negatively diagnosed patients. gRNA is written on the left side of the microplate. In the presence of COVID-19 patient samples, the color of all dCas9/gRNA (CoV-2 N1, N2, and N3)-immobilized wells turns yellow.

■ ASSOCIATED CONTENT

Supporting Information

The Supporting Information is available free of charge at https://pubs.acs.org/doi/10.1021/acssensors.0c01929.

Binding of RNA and biotin-PAMmer with the dCas9/gRNA complex (Figure S1); dCas9/gRNA RNP complex immobilization on the surface (Figure S2); optimization of the colorimetric RNA detection method (Figure S3); detection of SARS-CoV-2 N1 and pH1N1 H1 RNAs using CRISPR/dCas9 (Figure S4); detection of SARS-CoV-2 N2 and N3 RNAs using CRISPR/dCas9 (Figure S5); single nucleotide discrimination using perfectly matched gRNA (Figure S6); colorimetric virus detection using CRISPR/dCas9 (Figure S7); sequence information (Table S1); qPCR results of COVID-19 patients (Table S2); and comparison with other CRISPR/Cas system-based virus detection methods (Table S3) (PDF)

■ AUTHOR INFORMATION

Corresponding Authors

Juyeon Jung − *Bionanotechnology Research Center, KRIBB, Daejeon 34141, Republic of Korea; Department of Nanobiotechnology, KRIBB School of Biotechnology, UST, Daejeon 34113, Republic of Korea*; Email: jjung@kribb.re.kr

Hyun Gyu Park − *Department of Chemical and Biomolecular Engineering, KAIST, Daejeon 34141, Republic of Korea*; orcid.org/0000-0001-9978-3890; Email: hgpark1@kaist.ac.kr

Taejoon Kang − *Bionanotechnology Research Center, KRIBB, Daejeon 34141, Republic of Korea*; orcid.org/0000-0002-5387-6458; Email: kangtaejoon@kribb.re.kr

Authors

Jeong Moon − *Bionanotechnology Research Center, KRIBB, Daejeon 34141, Republic of Korea; Department of Chemical and Biomolecular Engineering, KAIST, Daejeon 34141, Republic of Korea*

Hyung-Jun Kwon − *Functional Biomaterial Research Center, KRIBB, Daejeon 34141, Republic of Korea*

Dongeun Yong − *Department of Laboratory Medicine and Research Institute of Bacterial Resistance, Yonsei University College of Medicine, Seoul 03722, Republic of Korea*

In-Chul Lee − *Functional Biomaterial Research Center, KRIBB, Daejeon 34141, Republic of Korea*

Hongki Kim − *Bionanotechnology Research Center, KRIBB, Daejeon 34141, Republic of Korea*

Hyunju Kang − *Bionanotechnology Research Center, KRIBB, Daejeon 34141, Republic of Korea*

Eun-Kyung Lim − *Bionanotechnology Research Center, KRIBB, Daejeon 34141, Republic of Korea; Department of Nanobiotechnology, KRIBB School of Biotechnology, UST, Daejeon 34113, Republic of Korea*; orcid.org/0000-0003-2793-3700

Kyu-Sun Lee − *Bionanotechnology Research Center, KRIBB, Daejeon 34141, Republic of Korea*

Complete contact information is available at: https://pubs.acs.org/10.1021/acssensors.0c01929

Notes

The authors declare no competing financial interest.

■ ACKNOWLEDGMENTS

This research was supported by the Basic Science Research Program through the National Research Foundation of Korea (NRF) funded by the Ministry of Science and ICT (MSIT) (NRF-2019R1C1C1006867 and NRF-2020R1A2C1010453), the Center for BioNano HealthGuard funded by the MSIT of Korea as a Global Frontier Project (H-GUARD_2013-M3A6B2078950 and H-GUARD_2014M3A6B2060507), the Bio & Medical Technology Development Program of the NRF funded by the MSIT of Korea (NRF-2018M3A9E2022821), KRIBB Research Initiative Program, and Kyung Nam Pharm. and Kyung Nam Biopharma. J.M. is a recipient of the Global Ph.D. Fellowship (NRF-2019H1A2A1073468).

■ REFERENCES

(1) Wang, C.; Horby, P. W.; Hayden, F. G.; Gao, G. F. A novel coronavirus outbreak of global health concern. *Lancet* **2020**, *395*, 470−473.

(2) Zhu, N.; Zhang, D.; Wang, W.; Li, X.; Yang, B.; Song, J.; Zhao, X.; Huang, B.; Shi, W.; Lu, R.; Niu, P.; Zhan, F.; Ma, X.; Wang, D.; Xu, W.; Wu, G.; Gao, G. F.; Tan, W. A Novel Coronavirus from Patients with Pneumonia in China, 2019. *N. Engl. J. Med.* **2020**, *382*, 727−733.

(3) WHO Coronavirus Disease (COVID-2019) Situation Reports, 2020. https://www.who.int/emergencies/diseases/novel-coronavirus-2019/situation-reports.

(4) Grein, J.; Ohmagari, N.; Shin, D.; Diaz, G.; Asperges, E.; Castagna, A.; Feldt, T.; Green, G.; Green, M. L.; Lescure, F. X.; Nicastri, E.; Oda, R.; Yo, K.; Quiros-Roldan, E.; Studemeister, A.; Redinski, J.; Ahmed, S.; Bernett, J.; Chelliah, D.; Chen, D.; Chihara, S.; Cohen, S. H.; Cunningham, J.; D'Arminio Monforte, A.; Ismail, S.; Kato, H.; Lapadula, G.; L'Her, E.; Maeno, T.; Majumder, S.; Massari, M.; Mora-Rillo, M.; Mutoh, Y.; Nguyen, D.; Verweij, E.; Zoufaly, A.; Osinusi, A. O.; DeZure, A.; Zhao, Y.; Zhong, L.; Chokkalingam, A.; Elboudwarej, E.; Telep, L.; Timbs, L.; Henne, I.; Sellers, S.; Cao, H.; Tan, S. K.; Winterbourne, L.; Desai, P.; Mera, R.; Gaggar, A.; Myers, R. P.; Brainard, D. M.; Childs, R.; Flanigan, T. Compassionate Use of Remdesivir for Patients with Severe Covid-19. *N. Engl. J. Med.* **2020**, *382*, 2327−2336.

(5) Seo, G.; Lee, G.; Kim, M. J.; Baek, S. H.; Choi, M.; Ku, K. B.; Lee, C. S.; Jun, S.; Park, D.; Kim, H. G.; Kim, S. J.; Lee, J. O.; Kim, B.

T.; Park, E. C.; Kim, S. I. Rapid Detection of COVID-19 Causative Virus (SARS-CoV-2) in Human Nasopharyngeal Swab Specimens Using Field-Effect Transistor-Based Biosensor. *ACS Nano* **2020**, *14*, 5135−5142.
(6) Pokhrel, P.; Hu, C.; Mao, H. Detecting the Coronavirus (COVID-19). *ACS Sens.* **2020**, *5*, 2283−2296.
(7) Shrestha, S. S.; Swerdlow, D. L.; Borse, R. H.; Prabhu, V. S.; Finelli, L.; Atkins, C. Y.; Owusu-Edusei, K.; Bell, B.; Mead, P. S.; Biggerstaff, M.; Brammer, L.; Davidson, H.; Jernigan, D.; Jhung, M. A.; Kamimoto, L. A.; Merlin, T. L.; Nowell, M.; Redd, S. C.; Reed, C.; Schuchat, A.; Meltzer, M. I. Estimating the burden of 2009 pandemic influenza A (H1N1) in the United States (April 2009-April 2010). *Clin. Infect. Dis.* **2011**, *52*, S75−S82.
(8) Eom, G.; Hwang, A.; Kim, H.; Yang, S.; Lee, D. K.; Song, S.; Ha, K.; Jeong, J.; Jung, J.; Lim, E. K.; Kang, T. Diagnosis of Tamiflu-Resistant Influenza Virus in Human Nasal Fluid and Saliva Using Surface-Enhanced Raman Scattering. *ACS Sens.* **2019**, *4*, 2282−2287.
(9) Eom, G.; Hwang, A.; Lee, D. K.; Guk, K.; Moon, J.; Jeong, J.; Jung, J.; Kim, B.; Lim, E.-K.; Kang, T. Superb Specific, Ultrasensitive, and Rapid Identification of the Oseltamivir-Resistant H1N1 Virus: Naked-Eye and SERS Dual-Mode Assay Using Functional Gold Nanoparticles. *ACS Appl. Bio Mater.* **2019**, *2*, 1233−1240.
(10) Hwang, S. G.; Ha, K.; Guk, K.; Lee, D. K.; Eom, G.; Song, S.; Kang, T.; Park, H.; Jung, J.; Lim, E. K. Rapid and simple detection of Tamiflu-resistant influenza virus: Development of oseltamivir derivative-based lateral flow biosensor for point-of-care (POC) diagnostics. *Sci. Rep.* **2018**, *8*, No. 12999.
(11) CDC Real-time RT−PCR Panel for Detection 2019-nCoV (US Centers for Disease Control and Prevention, 2020), 2020. https://www.cdc.gov/coronavirus/2019-ncov/lab/rt-pcr-detection-instructions.html.
(12) Broughton, J. P.; Deng, X.; Yu, G.; Fasching, C. L.; Servellita, V.; Singh, J.; Miao, X.; Streithorst, J. A.; Granados, A.; Sotomayor-Gonzalez, A.; Zorn, K.; Gopez, A.; Hsu, E.; Gu, W.; Miller, S.; Pan, C. Y.; Guevara, H.; Wadford, D. A.; Chen, J. S.; Chiu, C. Y. CRISPR-Cas12-based detection of SARS-CoV-2. *Nat. Biotechnol.* **2020**, *38*, 870−874.
(13) Zhang, W.; Du, R. H.; Li, B.; Zheng, X. S.; Yang, X. L.; Hu, B.; Wang, Y. Y.; Xiao, G. F.; Yan, B.; Shi, Z. L.; Zhou, P. Molecular and serological investigation of 2019-nCoV infected patients: implication of multiple shedding routes. *Emerging Microbes Infect.* **2020**, *9*, 386−389.
(14) Morales-Narváez, E.; Dincer, C. The impact of biosensing in a pandemic outbreak: COVID-19. *Biosens. Bioelectron.* **2020**, *163*, No. 112274.
(15) Cui, F.; Zhou, H. S. Diagnostic methods and potential portable biosensors for coronavirus disease 2019. *Biosens. Bioelectron.* **2020**, *165*, No. 112349.
(16) Barrangou, R.; Marraffini, L. A. CRISPR-Cas systems: Prokaryotes upgrade to adaptive immunity. *Mol. Cell* **2014**, *54*, 234−244.
(17) Moon, S. B.; Kim, D. Y.; Ko, J. H.; Kim, Y. S. Recent advances in the CRISPR genome editing tool set. *Exp. Mol. Med.* **2019**, *51*, 1−11.
(18) Chen, J. S.; Ma, E.; Harrington, L. B.; Da Costa, M.; Tian, X.; Palefsky, J. M.; Doudna, J. A. CRISPR-Cas12a target binding unleashes indiscriminate single-stranded DNase activity. *Science* **2018**, *360*, 436−439.
(19) Chiu, C. Cutting-Edge Infectious Disease Diagnostics with CRISPR. *Cell Host Microbe* **2018**, *23*, 702−704.
(20) Gootenberg, J. S.; Abudayyeh, O. O.; Lee, J. W.; Essletzbichler, P.; Dy, A. J.; Joung, J.; Verdine, V.; Donghia, N.; Daringer, N. M.; Freije, C. A.; Myhrvold, C.; Bhattacharyya, R. P.; Livny, J.; Regev, A.; Koonin, E. V.; Hung, D. T.; Sabeti, P. C.; Collins, J. J.; Zhang, F. Nucleic acid detection with CRISPR-Cas13a/C2c2. *Science* **2017**, *356*, 438−442.
(21) Guk, K.; Keem, J. O.; Hwang, S. G.; Kim, H.; Kang, T.; Lim, E. K.; Jung, J. A facile, rapid and sensitive detection of MRSA using a CRISPR-mediated DNA FISH method, antibody-like dCas9/sgRNA complex. *Biosens. Bioelectron.* **2017**, *95*, 67−71.
(22) Li, S. Y.; Cheng, Q. X.; Wang, J. M.; Li, X. Y.; Zhang, Z. L.; Gao, S.; Cao, R. B.; Zhao, G. P.; Wang, J. CRISPR-Cas12a-assisted nucleic acid detection. *Cell Discovery* **2018**, *4*, 20.
(23) Myhrvold, C.; Freije, C. A.; Gootenberg, J. S.; Abudayyeh, O. O.; Metsky, H. C.; Durbin, A. F.; Kellner, M. J.; Tan, A. L.; Paul, L. M.; Parham, L. A.; Garcia, K. F.; Barnes, K. G.; Chak, B.; Mondini, A.; Nogueira, M. L.; Isern, S.; Michael, S. F.; Lorenzana, I.; Yozwiak, N. L.; MacInnis, B. L.; Bosch, I.; Gehrke, L.; Zhang, F.; Sabeti, P. C. Field-deployable viral diagnostics using CRISPR-Cas13. *Science* **2018**, *360*, 444−448.
(24) Xiong, Y.; Zhang, J.; Yang, Z.; Mou, Q.; Ma, Y.; Xiong, Y.; Lu, Y. Functional DNA Regulated CRISPR-Cas12a Sensors for Point-of-Care Diagnostics of Non-Nucleic-Acid Targets. *J. Am. Chem. Soc.* **2020**, *142*, 207−213.
(25) Zhou, W.; Hu, L.; Ying, L.; Zhao, Z.; Chu, P. K.; Yu, X. F. A CRISPR-Cas9-triggered strand displacement amplification method for ultrasensitive DNA detection. *Nat. Commun.* **2018**, *9*, No. 5012.
(26) Li, Y.; Li, S.; Wang, J.; Liu, G. CRISPR/Cas Systems towards Next-Generation Biosensing. *Trends Biotechnol.* **2019**, *37*, 730−743.
(27) Choi, Y.; Hwang, J. H.; Lee, S. Y. Recent Trends in Nanomaterials-Based Colorimetric Detection of Pathogenic Bacteria and Viruses. *Small Methods* **2018**, *2*, No. 1700351.
(28) Oh, S.; Kim, J.; Tran, V. T.; Lee, D. K.; Ahmed, S. R.; Hong, J. C.; Lee, J.; Park, E. Y.; Lee, J. Magnetic Nanozyme-Linked Immunosorbent Assay for Ultrasensitive Influenza A Virus Detection. *ACS Appl. Mater. Interfaces* **2018**, *10*, 12534−12543.
(29) Jinek, M.; Chylinski, K.; Fonfara, I.; Hauer, M.; Doudna, J. A.; Charpentier, E. A programmable dual-RNA-guided DNA endonuclease in adaptive bacterial immunity. *Science* **2012**, *337*, 816−821.
(30) Nelles, D. A.; Fang, M. Y.; O'Connell, M. R.; Xu, J. L.; Markmiller, S. J.; Doudna, J. A.; Yeo, G. W. Programmable RNA Tracking in Live Cells with CRISPR/Cas9. *Cell* **2016**, *165*, 488−496.
(31) Azevedo, A. M.; Martins, V. C.; Prazeres, D. M.; Vojinovic, V.; Cabral, J. M.; Fonseca, L. P. Horseradish peroxidase: a valuable tool in biotechnology. *Biotechnol. Annu. Rev.* **2003**, *9*, 199−247.
(32) Spencer, S. M.; Lin, L.; Chiang, C. F.; Peng, Z.; Hesketh, P.; Salon, J.; Huang, Z. Direct and rapid detection of RNAs on a novel RNA microchip. *ChemBioChem* **2010**, *11*, 1378−1382.
(33) Zhou, L.; Peng, R.; Zhang, R.; Li, J. The applications of CRISPR/Cas system in molecular detection. *J. Cell. Mol. Med.* **2018**, *22*, 5807−5815.
(34) WHO Information for Molecular Diagnosis of Influenza Virus, 2020. https://www.who.int/influenza/gisrs_laboratory/molecular_diagnosis/en/.
(35) Jeong, M. S.; Ahn, D. R. A microwell plate-based multiplex immunoassay for simultaneous quantitation of antibodies to infectious viruses. *Analyst* **2015**, *140*, 1995−2000.
(36) Kaul, K. L.; Mangold, K. A.; Du, H.; Pesavento, K. M.; Nawrocki, J.; Nowak, J. A. Influenza A subtyping: seasonal H1N1, H3N2, and the appearance of novel H1N1. *J. Mol. Diagn.* **2010**, *12*, 664−669.
(37) Doench, J. G.; Fusi, N.; Sullender, M.; Hegde, M.; Vaimberg, E. W.; Donovan, K. F.; Smith, I.; Tothova, Z.; Wilen, C.; Orchard, R.; Virgin, H. W.; Listgarten, J.; Root, D. E. Optimized sgRNA design to maximize activity and minimize off-target effects of CRISPR-Cas9. *Nat. Biotechnol.* **2016**, *34*, 184−191.
(38) Carr, M. J.; Sayre, N.; Duffy, M.; Connell, J.; Hall, W. W. Rapid molecular detection of the H275Y oseltamivir resistance gene mutation in circulating influenza A (H1N1) viruses. *J. Virol. Methods* **2008**, *153*, 257−262.
(39) Lin, Y.; Cradick, T. J.; Brown, M. T.; Deshmukh, H.; Ranjan, P.; Sarode, N.; Wile, B. M.; Vertino, P. M.; Stewart, F. J.; Bao, G. CRISPR/Cas9 systems have off-target activity with insertions or deletions between target DNA and guide RNA sequences. *Nucleic Acids Res.* **2014**, *42*, 7473−7485.
(40) Ackerman, C. M.; Myhrvold, C.; Thakku, S. G.; Freije, C. A.; Metsky, H. C.; Yang, D. K.; Ye, S. H.; Boehm, C. K.; Kosoko-

https://dx.doi.org/10.1021/acssensors.0c01929
ACS Sens. XXXX, XXX, XXX−XXX

Thoroddsen, T. F.; Kehe, J.; Nguyen, T. G.; Carter, A.; Kulesa, A.; Barnes, J. R.; Dugan, V. G.; Hung, D. T.; Blainey, P. C.; Sabeti, P. C. Massively multiplexed nucleic acid detection using Cas13. *Nature* **2020**, *582*, 277−282.
(41) Liu, J.; Liao, X.; Qian, S.; Yuan, J.; Wang, F.; Liu, Y.; Wang, Z.; Wang, F. S.; Liu, L.; Zhang, Z. Community Transmission of Severe Acute Respiratory Syndrome Coronavirus 2, Shenzhen, China, 2020. *Emerging Infect. Dis.* **2020**, *26*, 1320−1323.
(42) KCDC The Updates on COVID-19 in Korea, 2020. https://www.cdc.go.kr/board/board.es?mid=a30402000000&bid=0030.

https://dx.doi.org/10.1021/acssensors.0c01929
ACS Sens. XXXX, XXX, XXX−XXX